$Cu(In_{1-x},Ga_x)Se_2$ THIN FILM SOLAR CELLS USING TRANSPARENT CONDUCTING OXIDE BACK CONTACTS FOR BIFCIAL AND TANDEM SOLAR CELLS

T. Nakada, Y. Hirabayashi, T. Tokado and D.Ohmori
Department of Electrical Engineering and Electronics, Aoyama Gakuin University,
5-10-1 Fuchinobe, Sagamihara, Kanagawa, 229-8558, Japan
TEL:++81-42-754-6251, FAX: +81-042-754-6521, E-mail: nakada@ee.aoyama.ac.jp

ABSTRACT

$Cu(In_{1-x},Ga_x)Se_2$ (CIGS)-based thin film solar cells have been fabricated using transparent conducting oxide (TCO) back contacts allowing light to pass through the entire solar cell structure. The cell performance of CIGS devices using tin oxide (SnO_2) and indium tin oxide (ITO) back contacts were almost the same as that of a conventional CIGS solar cell fabricated using a Mo back contact. In contrast, fairly low efficiency was achieved for a device fabricated using a ZnO:Al back contact. The best cell performance was obtained using a substrate temperatures of 500-520℃. However, the cell performance was observed to deteriorate above 550℃. This is attributed to increased resistivity of the TCO's due to the outdiffusion of fluorine dopant atoms from SnO_2 and the formation of a Ga_2O_3 interfacial layer on the ITO layer. We propose a low-cost bifacial CIGS thin film solar cell for the first time as one of the key applications of this type of CIGS device; preliminary results of cell performance are presented. A four-terminal tandem CIGS solar cell is also briefly discussed.

1. INTRODUCTION

For conventional $Cu(In,Ga)Se_2$ thin film solar cells, metallic Mo back electrodes are commonly used, making it impossible for light to pass through the metal electrode layer. However, a semitransparent solar cell is required for the top cell of multijunction (tandem) devices and in addition such a cell has the potential for use in applications such as bifacial devices and solar windows.

We thus have investigated an alternative structure for CIGS-based thin film solar cells using transparent conducting oxide (TCO) back contacts in which light can pass through the entire solar cell structure [1]. NREL [2] and HMI [3] groups have also reported similar cell structures and demonstrated four-terminal tandem devices. However, several problems still remain before high efficiency CIGS-based tandem solar cells including a low efficiency top cell fabricated using $CuGaSe_2$ or other wide-gap chalcogenide solar cells can be achieved. Another problem is the increased manufacturing costs of producing a complicated cell structure as compared to a single junction device. We therefore propose a bifacial CIGS thin film solar cell as a candidate for a low-cost high efficiency CIGS solar cell. In this paper, the details of the fabrication and performance of CIGS thin film solar cells using TCO back contacts are first described. Preliminary results on bifacial CIGS devices are then presented.

2. CELL STRUCTURE AND FABRICATION

Figure 1(a) shows the cell structure of a CIGS-based thin film solar cell using an n^+ type transparent conducting oxide (TCO) back contact as an alternative to a metallic Mo thin film. This type

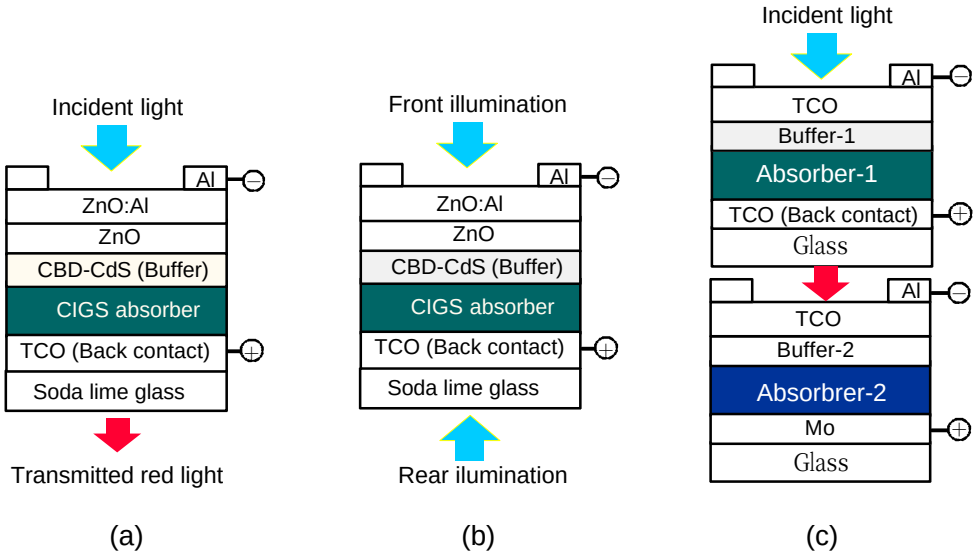

Fig. 1. (a) Cell structure of a CIGS-based thin film solar cell using an n^+-type TCO back contact alternative to a metallic Mo thin film, (b) bifacial CIGS solar cell, and (c) four-terminal tandem solar cell.

of cell can be considered to be a basic unit of both bifacial and tandem devices as shown in Fig. 1(b) and (c), respectively. In this work, commercially available F-doped tin oxide (SnO_2:F) was mainly used. The sheet resistance and optical transmission of the SnO_2:F were 7 ohm/sq and more than 85% at 550 nm, respectively. Indium tin oxide (ITO) thin films were also used for additional experiments. The sheet resistance and optical transmission were 10 ohm/sq and more than 85% at 550 nm, respectively. The detailed performance of devices using ITO back contacts has been reported elsewhere [4]. CIGS thin films were deposited by the three-stage process onto TCO-coated glass substrates at growth temperatures of 400-550℃. The film composition of CIGS thin film measured by inductively coupled plasma spectroscopy (ICP) was typically Cu:In:Ga:Se=23.20:16.54:9.20:51.07, Ga/(In+Ga)=0.36, Cu/(In+Ga)=0.90 and Se/metal=1.04. Wide-gap $CuGaSe_2$ thin films were deposited by a method similar to CIGS deposition excluding the In evaporation step. The film composition was determined to be Cu:Ga:Se=23.9:25.6:50.5, Cu/Ga=0.93 and Se/(Cu+Ga)=1.02. A CBD-CdS buffer layer was then deposited onto the CIGS or CGS absorber layers using a $CdSO_4$ (0.16 M)-ammonia (7.5 M)-thiourea (0.6 M) aqueous solution at 80℃. Non-doped ZnO and transparent conducting ZnO:Al thin films were then subsequently deposited using rf magnetron sputtering at room temperature. Current-voltage (J-V) characteristics were measured using a solar simulator calibrated by a Si standard cell guaranteed by the Japan Quality Association (JQA) under AM 1.5, 100 mW/cm^2 illumination at 24℃.

3. CELL PERFORMANCE

Figure 2(a) shows J-V characteristics of (a) CIGS, (b) CGS thin film solar cells fabricated using SnO_2 back contacts, and (c) conventional CIGS thin film solar cell fabricated using Mo back contact, indicating a best efficiency of 13.7% with V_{oc}=608 mV, J_{sc}=36.1 mA/cm^2, FF=0.626, and an active area of 0.2 cm^2. The cell performance was almost the same as that of a conventional CIGS thin film solar cell fabricated using a Mo back electrode as can be seen in Fig. 2(c). We have also fabricated CGS thin film solar cells using a SnO_2 back electrode formed by a similar process. However, CGS devices at present show a poor cell performance as shown in Fig. 2(b), indicating an efficiency of 3.3 % with V_{oc}=0.530, J_{sc}=14.0 mA/cm^2, and FF=0.450. The spectral response curves of the same devices are shown in Fig. 3 (a). The fall-off at long wavelengths of the spectral response curves corresponds to the band-gap energies of the absorber layers (780 nm for the CGS device and 1100 nm for CIGS devices). The quantum efficiency (QE) loss of both devices in the wavelength range of 400-500 nm is caused by the optical absorption within the CBD-CdS buffer layer. The QE loss of CIGS device at wavelengths longer than 800 nm is mainly attributable to a small minority carrier diffusion length due to the poor crystalline quality of the CIGS thin film in addition to the free carrier absorption loss of the transparent conducting ZnO:Al thin film. No difference in the response curve was observed for devices fabricated on Mo/SLG substrates (not shown here). Figure 3(b) shows

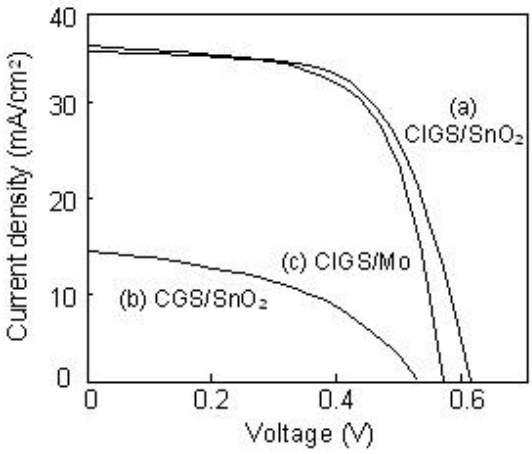

Fig. 2. J-V characteristics of (a) CIGS, (b) CGS thin film solar cells fabricated using SnO_2 back contacts, and (c) conventional CIGS thin film solar cell fabricated using Mo back contact.

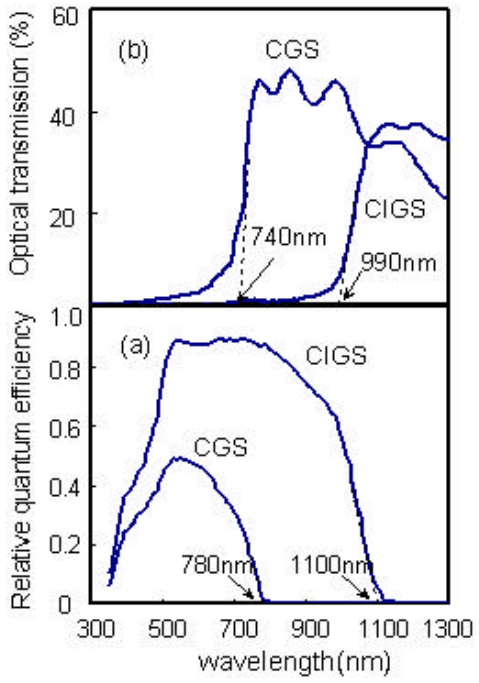

Fig. 3. The spectral response and optical transmission curves of the same devices shown in Fig.2.

the optical transmission curves of ZnO:Al/ZnO/CBD-CdS/CIGS/SnO_2/SLG and ZnO:Al/ZnO/CBD-CdS/CGS/SnO_2/SLG thin film solar cells shown in Fig. 3. The thicknesses of the absorber layers were 2 and 1 μm for the CIGS and CGS devices, respectively. It is evident that the optical transmission of the CGS solar cell rises at 740 nm and shows high transparency above this critical wavelength. This results in a semitransparent behavior in the red wavelength regions. In fact the CGS devices showed a brown-red transmission color. On the other hand, the CIGS solar cell

can generate the current using light in the wavelength range of 740-1100 nm. This result implies that a CGS thin film solar cell using TCO back contacts can be used in principle for the top cell of a CIGS-based tandem solar cell structure.

Similar experiments have been carried out for CIGS thin film solar cells fabricated using ITO and ZnO:Al back contacts. The substrate temperatures of CIGS deposition were 500℃ for SnO_2 and 520℃ for ITO and ZnO:Al coated substrates. Table I summarizes the cell performance of CIGS thin film solar cells fabricated using SnO_2, ITO and ZnO:Al back contacts. Data on conventional CIGS devices with Mo back contacts that was prepared simultaneously are also tabulated for comparison. As can be seen from the table, almost the same cell performance was obtained for all three types of CIGS thin film solar cells. In contrast, fairly low efficiency was achieved for a device fabricated using a ZnO:Al back contact. This may be interpreted as being due to interdiffusion or the formation of an intermediate layer at the CIGS/ZnO:Al interface after CIGS deposition at high substrate temperatures. Table II summarizes the preliminary results of the cell performance of CGS thin film solar cells fabricated using SnO_2 and ITO back contacts. The CGS thin film solar cell fabricated using an ITO back contact showed an efficiency of 4.0% with V_{oc}=673 mV, J_{sc}=13.4 mA/cm^2 and FF=0.438. The V_{oc} and FF were relatively low as compared to values reported for conventional CGS cells. Assuming the efficiency of the bottom cell is 1/4 that of the CIGS device [3], approximately 7 % efficiency could be obtained for a four-terminal tandem solar cell by adding in the 4% efficiency of the top CGS cell.

Table I. Cell performance of CIGS thin film solar cells fabricated using SnO_2, ITO, ZnO:Al and Mo back contacts.

Back contacts	V_{oc} (mV)	Jsc (mA/cm^2)	FF	Eff (%)
SnO_2	608	36.1	0.626	13.7
	590	36.9	0.624	13.6
ITO	568	35.1	0.652	13.0
	602	35.2	0.652	13.8
ZnO:Al	267	0.45	0.269	0.04
Mo	542	36.7	0.662	13.2
	565	36.8	0.643	13.3

Table II. Cell performance of CGS thin film solar cells fabricated using SnO_2 and ITO back contacts.

Back contact	V_{oc} (mV)	J_{sc} (mA/cm^2)	FF	η (%)
SnO_2	534	12.6	0.470	3.2
	528	14.0	0.446	3.3
ITO	673	13.4	0.438	4.0
	605	14.5	0.459	4.0

4. THE DEPENDENCE OF CELL PERFORMANCE ON GROWTH TEMPERATURE

Figure 4 shows the dependence of cell performance on substrate temperature during CIGS deposition for devices fabricated using a SnO_2 back contact. As can be seen from the figure, cell efficiency increased as the substrate temperature increased to 500℃. This can be interpreted as being a result of improved crystallinity of the CIGS absorber layer.

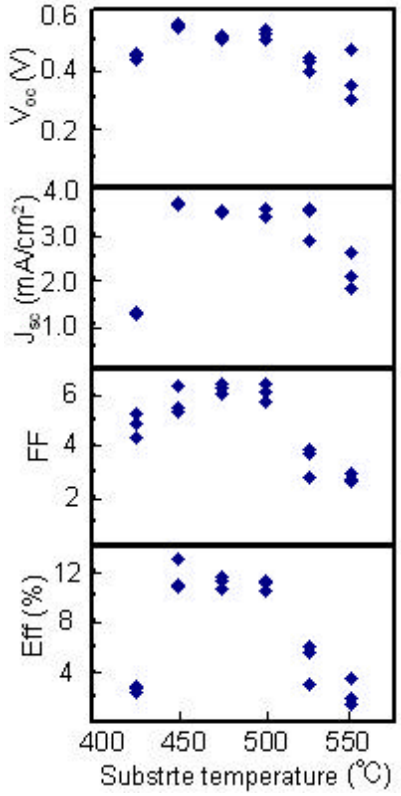

Fig. 4. The dependence of cell performance on substrate temperature during CIGS deposition for devices fabricated using a SnO_2 back contact.

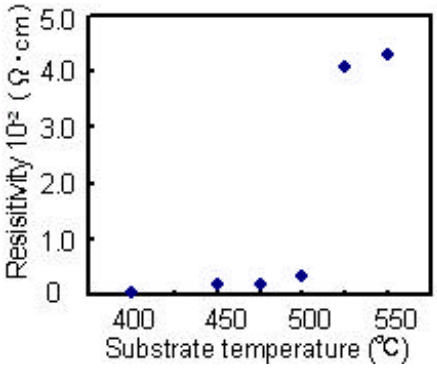

Fig. 5. The resistivity of SnO_2 layer after CIGS deposition at verious substrate temperatures.

On the other hand, The efficiency rapidly decreased above 525℃ mainly due to a decrease in fill factor (FF). The decreased in the FF is attributable to an increase in resistivity of the SnO_2 back contact after CIGS deposition as can be seen in Fig. 5.

In order to reveal the cause SIMS analysis was carried out for CIGS/SnO_2 stacked layers with various CIGS deposition temperatures. As a result it was found that the fluorine content decreased throughout the SnO_2:F layer after CIGS deposition at a substrate temperatures of 550℃ (not shown here). Therefore it is concluded that the increased resistivity of SnO_2 is due to the removal of fluorine during CIGS deposition at high temperatures. From TEM and EDS analyses it was also found that there was no significant interdiffusion at the CIGS/SnO_2 interface.

On the other hand, for the devices made using ITO back contacts the best cell performance was achieved at a CIGS deposition temperature of 520℃ [4], that is relatively higher than that of SnO_2. The resistivity of the surface rapidly increased at the substrate temperature above 550℃. This behavior was similar to that observed for SnO_2; however, the degradation mechanism is completely different as discussed below. From TEM and EDS analyses, it was found that approximately a 30nm-Ga_2O_3 layer was formed after CIGS deposition at 550℃. It is known that the Ga_2O_3 shows n-type conduction. Therefore, n-Ga_2O_3/p-type CIGS absorber layer may form a p-n junction that acts as a reverse junction opposing current from the main junction near the CIGS/buffer region. This barrier deteriorates cell performance of CIGS thin film solar cells due to the formation of a double junction.

5. BIFACIAL CIGS THIN FILM SOLARCELLS

The bifacial CIGS thin film solar cell structure is shown in Fig. 1(b); the structure is similar to a basic CIGS solar cell shown in Fig. 1 (a) except for a relatively thin absorber layer and the grading of Ga content. Figure 6 shows the J-V characteristics of the device with a 1.5 μm-thick CIGS layer, measured under AM 1.5 illumination from the front and rear sides of the solar cell.

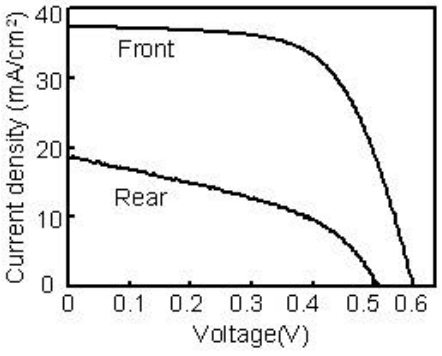

Fig. 6. J-V characteristics of the bifacial CIGS solar cell with a 1.5 μm-thick CIGS layer, measured under AM 1.5 illumination from the front and rear sides of the device.

The spectral response curves are also shown in Fig. 7. It is clear that the relative quantum efficiency (QE) at short wavelengths decreases for rear illumination. This is attributable in part to a large absorption loss at the rear-surface of CIGS absorber layer. Another possible reason is that the photo-generated carriers can't reach the junction area near the CIGS/buffer region. Table III summarizes the preliminary results of the cell performance of bifacial CIGS devices fabricated using an ITO back contact. As can be found from the table, cell performance measured under rear illumination improved for a cell (No.030131) with decreased thickness of CIGS absorber (0.5 μm) and optimized Ga grading. It is known that the contribution in efficiency from rear illumination is approximately 30% for the Si bifacial cells. Therefore similar increase in cell efficiency is expected for a practical usage. The details of this structure cell will be presented elsewhere.

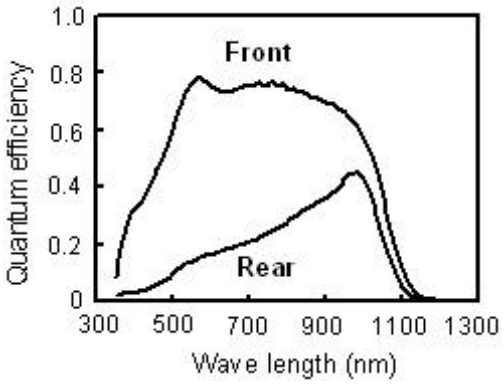

Fig. 7. The spectral response curves of the same device shown in Fig. 6.

Table III. Cell perforomance of bifacial CIGS thin film solar cells

Cell No.	Illuminated Side	V_{OC} (V)	J_{SC} (mA/cm²)	FF	η (%)
030131	Front	0.540	28.9	0.556	8.7
	Rear	0.498	36.7	0.460	8.4
021102	Front	0.564	37.0	0.635	13.3
	Rear	0.506	18.7	0.423	4.0

6. OHMIC BEHAVIOR OF CIGS AND CGS/TCO CONTACTS

Figure 8 shows the dark current-voltage characteristics of Au/C(I)GS/TCO stacked layers, which were measured at room temperature in a vacuum. An approximately 500-nm-thick Au thin film was evaporated onto a C(I)GS/TCO/SLG stacked layer at room temperature to form an ohmic contact. As can clearly be seen in Fig 8, the C(I)GS/TCO contacts exhibited ohmic behavior.

CIGS in thin film form usually shows p-type conduction except in the Cu-poor surface region, and has

demonstrated ohmic behavior at the CIGS/Mo back electrode interface [5]. Therefore an n-type TCO back contact is thought to form a barrier toward the p-type CIGS absorber layer, which deteriorates the performance of a solar cell with a ZnO:Al/ZnO/CBD-CdS/CIGS/TCO structure due to the formation of a second diode. However, the n^+-TCO/p-type CIGS contact does not always form a barrier and has the possibility of forming ohmic contact, which is controlled by the parameters such as the work function of degenerated n^+-TCO, and the electron affinity and band-gap energy (or work function) of CIGS.

Therefore, the ohmic behavior shown in Fig. 8 can be explained by two possible carrier transport mechanisms. One is an ohmic contact of a p-CIGS/n^+-TCO interface, a direct recombination of holes in the valence band of CIGS and electrons in the conduction band of TCO. The second is tunnel-enhanced recombination or trap-assisted tunneling when a very thin barrier is formed inside of the p-CIGS at the p-CIGS/n^+-TCO interface.

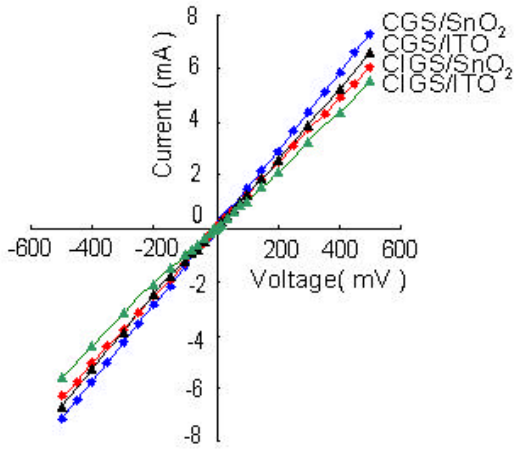

Fig. 8. Dark J-V characteristics of CIGS and CGS/TCO contacts at room temperature in a vacuum. Au thin film was evaporated onto CIGS and CGS for making ohmic contact.

CONCLUSIONS

$Cu(In_{1-x},Ga_x)Se_2$ (CIGS)-based thin film solar cells have been fabricated using transparent conducting oxide (TCO) back contacts. The cell performance of CIGS devices using SnO_2 and ITO back contacts was almost the same as that of conventional CIGS solar cell fabricated using Mo back metal electrodes. In contrast, fairly low efficiency was achieved for devices fabricated using a ZnO:Al back contact. The CIGS/TCO and CGS/TCO contacts showed ohmic behavior at room temperature. The best cell performance was obtained at substrate temperatures of 500-520℃. However, cell performance deteriorated above 550℃. This is attributable to increased resistivity of the TCO's due to the removal of fluorine from SnO_2 and the formation of a Ga_2O_3 thin layer on the ITO. We have proposed a low-cost bifacial CIGS thin film solar cell for the first time as a key application of semi-transparent CIGS devices. Although the cell conversion efficiency is not sufficient at present, it may be improved by optimization of bandgap engineering structures and layer thickness.

This work was supported in part by NEDO as a part of the New Sunshine Program.

REFERENCES

[1] T. Nakada, Y. Hirabayashi and T. Tokado : Jpn. J. Appl. Phys.Vol.41(2002)L1209-1211.
[2] D. L. Young, J. Abushama, R. Noufi, X. Li, J.Keane,T. A. Gessert, J. S. Ward, M. Contreras, M. Symko-Davies, and T. J. Coutts: Proc. 29th IEEE Photovolt. Specialists Conf. (2002)608-611.
[3] S. Nishiwaki, S. Siebentritt, P. Walk, and M. Ch. Lux-Steiner: Prog. Photovolt. (2003).
[4] T. Tokado an T.Nakada: This conference 2P-D3-66.

.